A Bisallylic Mini-lipoxygenase from Cyanobacterium *Cyanothece* sp. That Has an Iron as Cofactor*[S]

Alexandra Andreou[‡1]**, Cornelia Göbel**[‡]**, Mats Hamberg**[§]**, and Ivo Feussner**[‡2]

From the ‡Department of Plant Biochemistry, Albrecht von Haller Institute for Plant Sciences, Georg August University, Justus-von-Liebig-Weg 11, D-37077 Göttingen, Germany and the §Division of Chemistry II, Department of Medical Biochemistry and Biophysics, Karolinska Institutet, SE-17177 Stockholm, Sweden

Lipoxygenases are enzymes that are found ubiquitously in higher animals and plants, but have only recently been identified in a number of bacteria. The genome of the diazotrophic unicellular cyanobacterium *Cyanothece* sp. harbors two genes with homology to lipoxygenases. Here we describe the isolation of one gene, formerly named *csplox2*. It was cloned, and the protein was expressed in *Escherichia coli* and purified. The purified enzyme belongs to the group of prokaryotic mini lipoxygenases, because it had a molecular mass of 65 kDa. Interestingly, it catalyzed the conversion of linoleic acid, the only endogenously found polyunsaturated fatty acid, primarily to the bisallylic hydroperoxide 11R-hydroperoxyoctadecadienoic acid. This product had previously only been described for the manganese lipoxygenase from the take all fungus, *Gaeumannomyces graminis*. By contrast, CspLOX2 was shown to be an iron lipoxygenase. In addition, CspLOX2 formed a mixture of typical conjugated lipoxygenase products, *e.g.* 9R- and 13S-hydroperoxide. The conversion of linoleic acid took place with a maximum reaction rate of 31 s^{-1}. Incubation of the enzyme with [(11S)-²H]linoleic acid led to the formation of hydroperoxides that had lost the deuterium label, thus suggesting that CspLOX2 catalyzes antarafacial oxygenation as opposed to the mechanism of manganese lipoxygenase. CspLOX2 could also oxidize diarachidonylglycerophosphatidylcholine with similar specificity as the free fatty acid, indicating that binding of the substrate takes place with a "tail-first" orientation. We conclude that CspLOX2 is a novel iron mini-lipoxygenase that catalyzes the formation of bisallylic hydroperoxide as the major product.

Lipoxygenases (LOXs)[3] are non-heme iron or manganese-containing dioxygenases that catalyze the insertion of molecular oxygen into polyunsaturated fatty acids (PUFAs) with one or more (1Z,4Z)-pentadiene moieties leading to the formation of hydroperoxy PUFAs (1). LOXs are ubiquitously found in higher plants and animals, but have also been detected in some corals, mosses, fungi, and only recently, in a number of bacteria (2, 3).

LOX-derived fatty acid hydroperoxides can be further converted to produce important bioactive lipid mediators such as aldehydes and jasmonates in plants and leukotrienes, resolvins, and lipoxins in mammals. These signaling molecules play an important role in wound and defense responses as well as in aspects of plant development (3), whereas in mammals they function in inflammation, asthma, heart disease, and cancer (4–6). Information regarding the biological function of LOX products in fungi and prokaryotes is still scarce.

The active site metal of LOX is iron in the case of all as yet analyzed plant, animal, and bacterial enzymes and manganese in the case of a LOX from the take-all fungus *G. graminis*. The metal center undergoes redox cycles between the active, Fe^{3+} or Mn^{3+}, and inactive, Fe^{2+} or Mn^{2+}, form and residual hydroperoxides serve to reoxidize the metal. The metal is octahedrally coordinated by five amino acid residues, which are conserved throughout the kingdoms and consist of three histidines, an asparagine, and the C-terminal isoleucine (or valine) residue or in the case of some mammalian LOXs of four histidines and the isoleucine. A water or hydroxide may occupy the position of the sixth metal ligand (7).

The LOX reaction exhibits high regio- and stereospecificity. The reaction is initiated by the stereospecific abstraction of bisallylic hydrogen from the substrate, leading to the formation of a carbon centered radical. In the second step, oxygen is inserted with high regio- and stereospecificity. This oxygenation is antarafacial in the case of all LOXs, with the exception of manganese LOX (Mn-LOX). Here it has been reported to be suprafacial, possibly due to differences in the position of the oxygen access channel (8). In the case of plant LOXs, C18 fatty acids, linoleic (18:2(n-6)) and α-linolenic (18:3(n-3)) acids are the preferred substrates, and hydrogen abstraction takes place from C11. Oxygen insertion then occurs either in the (n-2) or in (n+2) position to produce either 9- or 13-hydroperoxides. Plant LOXs studied so far almost exclusively catalyze the insertion of oxygen with an *S* stereospecificity. 9R-products have

---

[3] The abbreviations used are: LOX, lipoxygenase; 16:1(n-7), palmitoleic acid; 18:1 (n-9), oleic acid; 18:2(n-6), linoleic acid; 18:3(n-3), α-linolenic acid; 20:4(n-6), arachidonic acid; 20:5(n-3), eicosapentaenoic acid; CP, chiral phase; CTAB, cetyltrimethylammonium bromide; diHPOTE, dihydroperoxyoctadecatrienoic acid; EPR, electron paramagnetic resonance; GC, gas chromatography; HPLC, high pressure liquid chromatography; H(P)ODE, hydro(pero)xyoctadecadienoic acid; H(P)OTE, hydro(pero)xyoctadecatrienoic acid; H(P)ETE, hydro(pero)xyeicosatetraenoic acid; ICP, inductively coupled plasma; KOTE, keto-octadecatrienoic acid; Mn-LOX, manganese lipoxygenase; MS, mass spectrometry; MS², tandem mass spectrometry; PC, phosphatidylcholine; PC-20:4(n-6), 1,2-diarachidonoyl-*sn*-glycero-3-phosphatidylcholine; RP, reversed phase; SP, straight phase; TIC, total ion current; PUFA, polyunsaturated fatty acid.

mainly been identified in cyanobacteria, whereas 13*R*-hydroperoxide has been reported to be one of the hydroperoxides produced by a dual specificity LOX from olive (9) and is the end product of the fungal Mn-LOX (10). The latter enzyme is also the only as yet characterized LOX that produces the bisallylic 11*S*-hydroperoxide. Here, the bisallylic 11*S*-hydroperoxide is an intermediate product, which can be further transformed to 13*R*-hydroperoxide.

The control of regio- and stereospecificity of the LOX reaction is still a matter of debate. Currently existing models, based on site-directed mutagenesis studies (11, 12) and the six available LOX structures from plants (13–17), mammals (18, 19), and coral (20, 21), have identified various, mostly non-polar, amino acid residues in the active site pocket that influence the regiospecificity of the LOX reaction catalyzed by a certain isozyme. In summary, the orientation and depth of substrate binding is predicted to play a role in determining the regiospecificity (7, 22). Stereospecificity has been reported to be controlled by a conserved amino acid residue, which is an alanine (or a serine) residue in *S*-LOXs and a glycine residue in most *R*-LOXs (1).

Prokaryotic and eukaryotic algae are known sources of biologically active compounds, such as fatty acid aldehydes, alcohols, and ketones, which may derive from primary products of LOX activity. As genome sequences of a number of cyanobacteria are being released, they become available for identifying and studying LOX enzymes of cyanobacterial origin by molecular tools. By searching the available genomic sequence of the unicellular nitrogen fixing cyanobacterium *Cyanothece* sp. for sequences that are similar to LOXs, we identified two putative LOX sequences (3). One of these putative enzymes (CspLOX2) was characterized biochemically. CspLOX2 belongs to the class of mini-LOXs, consisting only of the C-terminal catalytic domain, and is a novel LOX, because it forms bisallylic 11-hydroperoxide from 18:2(n-6) as a major product. The enzyme was found to contain iron and to otherwise follow a similar reaction mechanism to other iron LOXs with an initial stereospecific abstraction of the bisallylic pro-*S* hydrogen from C11 of 18:2(n-6) followed by an antarafacial oxygen attack at C11, C13, or C9.

EXPERIMENTAL PROCEDURES

Materials—Chemicals were obtained from Sigma and Carl Roth & Co. Agarose was from Biozym Scientific GmbH. All fatty acids were from Sigma or Cayman Chemical. 1,2-Diarachidonoyl-*sn*-glycero-3-phosphatidylcholine (PC-20:4(n-6)) was purchased from Avanti Polar Lipids, Inc. Acetonitrile was from Fisher Scientific. Restriction enzymes were purchased from MBI Fermentas. 9*R*-Hydroperoxyoctadecatrienoic acid (9*R*-HPOTE) and 9*R*-[U-^{13}C]HPOTE were prepared enzymatically from α-linolenic acid by ΔNt-NspLOX (23).

Isolation of 11R-Hydroxyoctadecadienoic Acid (HODE) Methyl Ester—Barley seeds were found to contain about 30 μg/g of 11*R*-HODE and thus serve as a convenient source of this rare oxylipin. Seeds of barley (100 g) were extracted with CHCl$_3$/MeOH (2:1, v/v) and the lipid extract treated with 0.4 M NaOH at 70 °C for 1 h. The product was purified by SiO$_2$ chromatography, then methyl-esterified and subjected to a second

SiO$_2$ chromatography (elution with diethyl ether/hexane (3:7, v/v)). The hydroxy ester fraction thus obtained was subjected to preparative reversed phase-HPLC (RP-HPLC; mobile phase, 65% aqueous acetonitrile) followed by straight phase-HPLC (SP-HPLC; mobile phase, 0.67% 2-propanol in hexane) to provide pure methyl (9*Z*,12*Z*)-11-hydroxy-9,12-octadecadienoate (1.3 mg), the structure of which was confirmed by mass spectrometry, Fourier transform infrared spectroscopy and chemical methods as previously described (24). An aliquot was subjected to partial hydrogenation, derivatization with ($-$)-menthoxycarbonyl chloride and oxidative ozonolysis. Analysis of the chiral cleavage fragments by gas chromatography (GC) demonstrated that the configuration of C11 was in the *R* configuration (optical purity, 90–91%).

Algal Material and Growth Conditions—*Cyanothece* sp. (PCC 8801) was obtained from the Pasteur Culture Collection of Cyanobacteria (PCC, Paris). Cultures were cultivated in BG11$_0$ medium for cyanobacteria (25) complemented with 5 mM of NaHCO$_3$ as inorganic carbon source according to the standard protocols of PCC using 1l conical flasks. The cultures were grown under constant illumination at a photosynthetic photon flux density of $\sim$35 μmol photons m^{-2} s^{-1}. After 3 weeks of cultivation, cells were harvested by centrifugation at 3220 $\times$ *g* for 10 min, and the pellets were stored at -20 °C.

Analysis of the Fatty Acid Composition of Cyanothece sp.— 0.4 g of freeze-dried cyanobacterial material was homogenized in 4 ml of *n*-hexane/2-propanol solution (3:2, v/v) with 0.0025% (w/v) 2-butyl-6-hydroxytoluene, to which 100 μg of heptadecanoic acid was added as internal standard, using a nitrogen-cooled Retsch MM200 mixer mill. The extract was shaken at 4 °C for 10 min and then centrifuged at 3200 $\times$ *g* at 4 °C for 10 min. To the clear upper phase, 3.1 ml of 6.7% (w/v) potassium sulfate solution were added to remove nonlipid contaminants. The sample was further incubated at 4 °C for 10 min under vigorous shaking, and the extract was then centrifuged at 3200 $\times$ *g* at 4 °C for 10 min. Subsequently, the upper hexane-rich layer was removed and dried under streaming nitrogen. The sample was resuspended in 200 μl of methanol, and 20 μl were used for determination of the free fatty acid composition. For this purpose methylated derivatives were produced by dissolving the sample in 400 μl of methanol containing 6.5 μl of 2 M (diazomethyl)trimethylsilane (in hexane). After incubation for 30 min under rigorous shaking, the reaction was terminated by the addition of 0.2 μl of glacial acid and solvent was removed by evaporation under streaming nitrogen. The sample was then dissolved in 10 μl of acetonitrile. Analysis of the fatty acid methyl esters was carried out using GC coupled to a flame ionization detector according to Ref. 26.

Cloning and Expression of Recombinant CspLOX2 in E. coli— Genomic DNA was isolated from approx. 50 mg of frozen cell material of *Cyanothece* sp. using the cetyltrimethylammonium bromide (CTAB) method with small modifications (27). The pellet was resuspended in 250 μl of CTAB-buffer (2% (w/v) CTAB, 100 mM Tris-HCl, pH 8, 20 mM EDTA pH 8, 1.4 M NaCl) with 2% (v/v) β-mercaptoethanol and was incubated at 65 °C for 3 h. Subsequently extraction was carried out with the addition of an equal volume of chloroform/isoamyl alcohol (24:1, v/v), 3 min of incubation, and centrifugation at 1100 $\times$ *g*. The

upper aqueous phase was mixed with 1/20 of the sample volume prewarmed CTAB/NaCl solution (10% CTAB-buffer, 0.7% (w/v) NaCl) and incubated at room temperature for 2 min. The samples were then centrifuged at 20,000 × g for 10 min. The supernatant was removed, and the precipitated DNA was washed with 100 μl of 75% (v/v) ethanol. After removal of the ethanol, the DNA was dried at room temperature and resuspended in water.

csplox2 (GenBank™ accession number YP_002373243) was amplified from genomic DNA with gene-specific primers containing BamHI and XhoI restriction sites (forward primer, 5′-CGGATCCATGGTACAACCAAGTTTACCCCAAG-3′; and reverse primer, 5′-GCTCGAGCTAAATACTGGTACTGTT-AGGGAC-3′) using PhusionTM High Fidelity DNA Polymerase (New England Biolabs). The PCR product was then cloned into the pJET vector (Fermentas) according to the manufacturer's instructions. The identity of the cloned gene was confirmed by DNA sequencing. The PCR product was further cloned into the pET28a expression vector (Merck). For heterologous expression of the His-tagged recombinant protein *E. coli* BL21 Star cells (Invitrogen) were grown in 2×YT containing 25 μg/ml kanamycin at 37 °C until an A_{600} of 1 and induced with the addition of 1 mM isopropyl β-D-thiogalactopyranoside. The cultures were additionally supplemented with 250 μM ammonium iron (III) citrate and further cultivated by shaking at 28 °C for 18 h. For purification of CspLOX2 frozen cell pellets from 600 ml of cultures were resuspended in 30 ml of 50 mM Tris, pH 7.5, 30 mM imidazole. Cells were incubated on ice for 30 min after the addition of 0.1 mg/ml lysozyme, 0.2 mM phenylmethylsulfonyl fluoride, 20 μg/ml DNase, and 1 mM MgCl₂. Cells were further disrupted by 3 pulses of 30-s sonication on ice, and the cell debris was centrifuged at 27,000 × g at 4 °C for 20 min. The supernatant was applied to a 1 ml of HisTrap FF column (GE Healthcare) previously equilibrated with 50 mM Tris, pH 7.5, 30 mM imidazole. The column was washed with the equilibration buffer, and the protein was finally eluted with 50 mM Tris, pH 7.5, 300 mM imidazole. Protein purity was evaluated by SDS-PAGE.

Measurement of Iron or Manganese Content of CspLOX2—The metal content of purified CspLOX2 was measured using inductively coupled plasma (ICP) atomic emission spectroscopy: The purified protein was concentrated and rebuffered to 10 mM HEPES pH 7.5 over a Spin-X UF concentrator (cutoff of 30,000, Corning). CspLOX2 was diluted to a final concentration of 24 μg/ml. ICP measurements were performed with a Spectro Flame (Spectro Analytical Instruments). The instrument was calibrated using standards of known iron or manganese concentration, and repeat measurements were reproducible within 5%. A blank buffer sample was measured in parallel with the protein sample.

LOX Activity Assay and HPLC Product Analysis—For activity assays, 15 μg of CspLOX2 were added to 900 μl of 0.2 M sodium borate buffer, pH 9.5 containing 250 μg of the respective substrate. The reaction was allowed to proceed at 23 °C for 30 min. Hydroperoxides formed were reduced to their corresponding hydroxides with addition of 900 μl of 50 mM SnCl₂, dissolved in methanol. After acidification to pH 3.0 with glacial acetic acid, fatty acids were extracted as described (28) and resuspended in

80 μl of acetonitrile/water/acetic acid (50:50:0.1, v/v/v) and subjected to HPLC analysis. Hydroxy fatty acids were separated from fatty acids with RP-HPLC using a EC250/2 Nucleosil 120−5 C₁₈ colum (250 × 2.1 mm, 5-μm particle size, Macherey-Nagel). Elution was carried out with a solvent system of: solvent A, acetonitrile/water/acetic acid (50:50:0.1, v/v/v); and solvent system B, acetonitrile/acetic acid (100:0.1, v/v) using the following gradient elution profile: flow rate of 0.18 ml/min, 0−5 min, 100% A; 5−20 min from 100% A to 100% B; 20−22 min flow rate increase to 0.36 ml/min; 22−27 min, 100% B; 27−32 min from 100% B to 100% A; and 32−35 min, 100% A, flow rate decreased to 0.18 ml/min. SP-HPLC of hydroxy fatty acid isomers was carried out on a Zorbax Rx-SIL column (150 × 2.1 mm, 5-μm particle size, Agilent) eluted with a solvent system of *n*-hexane/2-propanol/acetic acid (100:1:0.1, v/v/v) at a flow rate of 0.2 ml/min. Chiral phase-HPLC (CP-HPLC) of the hydroxy fatty acids was carried out on a Chiralcel OD-H column (150 × 2.1 mm, 5 μm particle size, Daicel, VWR) with a solvent system of *n*-hexane/2-propanol/trifluoroacetic acid (100:5:0.1, v/v/v) at a flow rate of 0.1 ml/min. Absorbance at 202 nm and 234 nm was recorded simultaneously for the detection of non-conjugated and conjugated hydroxy fatty acids, respectively, during all chromatographic steps. For separation of the stereoisomers of methylated 11-HODE a solvent system of *n*-hexane/2-propanol/trifluoroacetic acid (100:1:0.1, v/v/v) at a flow rate of 0.1 ml/min was used. Activity of CspLOX2 against phosphatidylcholine (PC) esters was measured by incubating 0.7 nmol of purified protein with 0.6 mg of PC-20:4(n-6) in 5 ml of 50 mM Tris, pH 9.5, 4 mM sodium deoxycholate under constant stirring at 23 °C for 30 min. Reduction of the hydroperoxides was performed as described above using SnCl₂. After chloroform evaporation, the lipid-bound fatty acids were converted to the corresponding methyl esters by adding 500 μl of 1% sodium methoxide solution and shaking at room temperature for 20 min. 500 μl of 6 M NaCl was added to the reaction, and the methyl esters were then extracted twice with 750 μl of hexane. The solvent was removed by evaporation under streaming nitrogen, and the sample was dissolved in 80 μl of methanol/water/acetic acid (75:25:0.1, v/v/v). Methyl esters were separated by RP-HPLC using a column as described above and with a solvent system of solvent A, methanol/water/acetic acid (75:25:0.1, v/v/v), and solvent B, methanol/acetic acid (100:0.1, v/v) using the following gradient: flow rate of 0.18 ml/min, 0−5 min, 100% A; 5−10 min from 100% A to 100% B, and flow rate increase to 0.36 ml/min; 10−20 min 100% B; 20−25 min from 100% B to 100% A; 25−30 min 100% A. SP-HPLC analysis was carried out using a column as described above with a solvent system of *n*-hexane/2-propanol/trifluoroacetic acid (100:1:0.02, v/v/v) at a flow rate of 0.1 ml/min. Quantification of the bisallylic product was accomplished by GC/MS analysis as described below.

HPLC/MS Analysis—Analysis was performed with a EC250/2 Nucleodur 100−5 C₁₈ column (250 × 2.1 mm, 5-μm particle size, Macherey-Nagel) and the following solvent system: solvent A, acetonitrile/water/acetic acid (40:60:0.1, v/v/v); and solvent B, acetonitrile/acetic acid (100:0.1, v/v). The gradient elution profile was as previously described (29). The effluent was then subjected to negative ion electrospray ionization in an

ion trap mass spectrometer (LCQ, Thermo Fisher Scientific). The capillary temperature was 300 °C, and the capillary voltage was 27 kV. In full scan mode, ions were collected between m/z values of 50 to 400. For tandem MS analysis, the collision energy was 1 V.

GC/MS Analysis—The identity of the hydroxy and dihydroxy fatty acids was verified by GC/MS. Samples were reduced with $SnCl_2$ and methylated as described above. Fatty acid methyl esters were dissolved in 3 μl of acetonitrile. Trimethylsilyl ester derivatives were prepared with sample treatment with 1 μl of *N,O*-bi(trimethylsilyl)trifluoroacetamide. Analysis was carried out using an Agilent 5973 mass selective detector coupled to an Agilent 6890 gas chromatograph equipped with a capillary column as described above. The temperature gradient was as described above for GC analysis of fatty acid composition.

Spectroscopy—Light absorbance was measured at room temperature using a Cary 100 Bio spectrophotometer (Varian). For incubations with 9-HPOTE, activity was measured by repetitive scanning in the range of 220–340 nm. 30 nM of purified enzyme was added to 1 ml of 0.2 M sodium borate, and the reaction was started with the addition of 9-HPOTE dissolved in ethanol.

Determination of the pH Optimum—The formation of the conjugated double bond of the 9-HPODE and 13-HPODE products at 234 nm ($\epsilon = 2.5 \times 10^4$ M^{-1} cm^{-1}) at a given pH using 100 μM sodium salt of 18:2(n-6) (30) as a substrate was monitored with a Cary 100 Bio spectrophotometer (Varian). The following buffers were used for the different pH ranges: 0.2 M acetate buffer (pH 4.5–5.5), 0.2 M phosphate buffer (pH 5.5–8.0), and 0.2 M borate buffer (pH 8.0–10.5). It was ensured that the different buffer systems did not influence enzyme activity.

Determination of Kinetic Parameters—For analysis of the initial reaction rate data, the time-dependent O_2 consumption was measured with a Clark-type O_2 electrode at different substrate concentrations. The kinetic experiments were conducted at 24 °C in 0.2 M sodium borate buffer pH 9.5. Reactions were initiated by the addition of 2 μg of purified enzyme to 1 ml of the rapidly stirring buffer containing a defined amount of substrate. The solution was pre-equilibrated against air at 1 atm. The kinetic parameters were calculated by nonlinear regression fitting of the experimental points to the Michaelis-Menten equation.

Labeled Substrate Synthesis—[(11S)-^{2}H]-18:2(n-6) was prepared according to Ref. 31. In short: chemical purity was >98%; isotope enrichment >98.0%; monodeuterated molecules and stereochemical purity of deuterium label >90%.

RESULTS

Cloning, Expression, and Purification of CspLOX2—BLAST search analysis of the *Cyanothece* sp. genome led to the identification of two DNA sequences encoding two putative LOXs, designated as CspLOX1 and CspLOX2 (3). Here the biochemical characterization of CspLOX2 will be described, while the activity of CspLOX1 will be reported separately. The deduced amino acid sequence showed that CspLOX2 consists only of a C-terminal catalytic LOX domain with highest homology to a putative arachidonate 15-LOX precursor from *Microcystis aeruginosa* and to NpLOX2, a linoleate 13-LOX from cya-
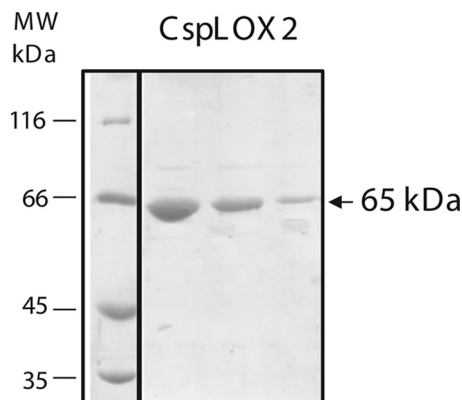

FIGURE 1. **SDS-PAGE analysis of the purified recombinant CspLOX2.** A single band migrating at ~65 kDa is visible in the elution fractions.

nobacterium *Nostoc punctiforme*. CspLOX2 showed 43% sequence identity and 60% similarity to the latter enzyme (32, 33). Alignment of the amino acid sequence revealed that CspLOX2 harbors the conserved metal ligands (3 histidine residues, an asparagine, and the C-terminal isoleucine), but not the residues described to play a role in determining regiospecificity in either mammalian or plant LOXs. The only described amino acid residue that appears to be conserved is an alanine, which aligns with a position that determines stereospecificity (supplemental Fig. S1). The full-length protein was cloned from *Cyanothece* sp. PCC 8801 genomic DNA into the expression vector pET28a. The protein was expressed in *Escherichia coli* in-frame with an N-terminal His$_6$ tag and purified by nickel affinity chromatography (Fig. 1). The final yield was 1 mg of CspLOX2 from 1 liter of culture. The purity of the protein was >90% as judged from SDS gel electrophoresis, where a single band at the molecular mass of ~65 kDa could be detected (Fig. 1). Measurement of the iron content of the purified protein by ICP gave an iron to protein ratio of 45%. In the same measurement, however, a manganese to protein ratio of 10% could also be observed. Addition of Fe^{3+} in the form of ammonium iron (III) citrate in the growth medium improved the expression of soluble protein significantly, resulting in a final yield of 20 mg of protein from 1 liter of culture. The iron content of the protein in this case was measured to be 92%, whereas the manganese to protein ratio was <2%. These results may indicate that CspLOX2 harbors iron in the active site, but low iron levels in the bacterial growth medium might lead to manganese incorporation.

Activity of CspLOX2—Analysis of the amount of free fatty acids of *Cyanothece* sp. revealed that the only PUFA and therefore potential endogenous LOX substrate present was 18:2(n-6), which represented 53% of the total free fatty acid amount. Other free fatty acids were 16:0, 16:1(n-7), 18:0 and 18:1(n-9) (Table 1). For initial characterization of CspLOX2, the pH optimum of the protein was investigated by measuring the initial rates of increase in absorption at 234 nm with 18:2(n-6) as substrate. CspLOX2 exhibited a very broad pH optimum, retaining over 50% of activity from pH 6–10, with an activity maximum at pH 9.3 (data not shown).

Identification of CspLOX2 Products—RP-HPLC/MS^2 analysis was carried out to analyze CspLOX2 reaction products

TABLE 1

Free fatty acid composition of *Cyanothece* sp. PCC 8801

Fatty acids were extracted from frozen cyanobacterial cells, methylated, and analysis of the methyl ester derivatives was performed via GC as described under "Experimental Procedures." The fatty acids were characterized by co-elution of authentic standards. The values presented here are the average of three independent measurements.

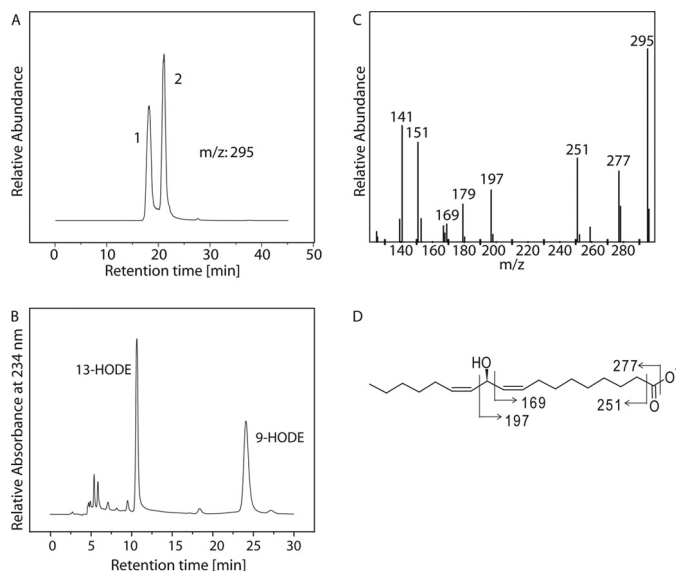| Fatty acid	Proportion of total fatty acids
	%
16:0	15.0
16:1(n-7)	7.8
18:0	9.1
18:1(n-9)	14.9
18:2(n-6)	53.2

FIGURE 2. **Product analysis formed from CspLOX2 with 18:2(n-6).** 250 μg of 18:2(n-6) were incubated with 15 μg of CspLOX2 for 30 min, and the reaction products were reduced by $SnCl_2$. *A*, RP-HPLC-MS^2 analysis of HODE (*top trace*, *m/z* 295 → full scan; *peak 1* contained 11-HODE and *peak 2* contained HODEs with conjugated double bond systems). *B*, SP-HPLC analysis of HODEs with conjugated double bond systems. *C*, MS^2 spectrum (*m/z* 295 → full scan) of 11-HODE. *D*, fragmentation pattern of 11-HODE and resulting fragment sizes.

formed with 18:2(n-6). Two peaks were detectable (Fig. 2*A*) with *m/z* of 295, corresponding to the molecular weight of HODE. The UV spectrum corresponding to peak 1 was featureless, whereas the mass spectrum matched the previously described spectrum of 11-HODE (34), with prominent ions at *m/z* 295 (M$^-$), 277 (M$^-$-18; loss of H_2O), 251 (M$^-$-44; loss of CO_2), 197 ($^-OOC(CH_2)_7CH = CHCHO$), 177, 169 ($^-OOC(CH_2)_7CH = CH_2$), 151 and 141 (Fig. 2, *C* and *D*). Under our assay conditions, 11-HODE was the main product of 18:2(n-6) transformation, comprising 39.2% of total detected products. Peak 2 showed an absorption maximum at 234 nm, which is characteristic for a conjugated diene system. By SP-HPLC analysis, peak 2 could be separated into two products, which were identified as 13- and 9-HODE (Fig. 2*B*). 9-HODE comprised 33.5% and 13-HODE 27.3% of total reaction products. The enantiomers of all HODEs were further resolved using CP-HPLC. The reduced conjugated hydroxide products of CspLOX2 were identified as 13*S*-HODE and 9*R*-HODE (Fig. 3, *B* and *C*). The bisallylic HODE was methylated before CP-HPLC analysis and identified as 11*R*-HODE (Fig. 3*A*).
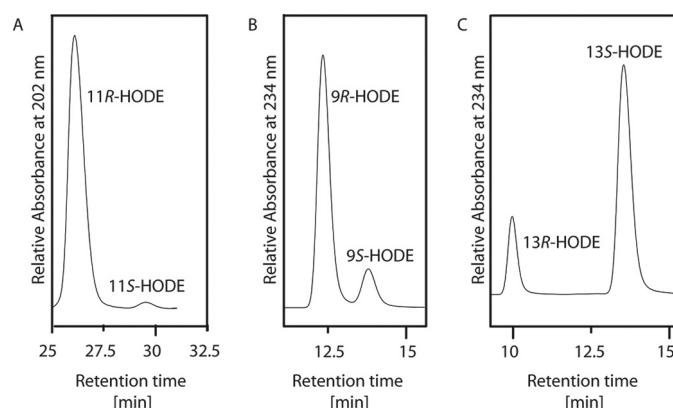

FIGURE 3. **CP-HPLC analysis of the HODE isomers produced by CspLOX2.** Product hydroxides were analyzed using a Chiralcel OD-H column (150 × 2.1 mm, 5-μm particle size, Daicel, VWR). *A*, analysis of 11-HODE methyl ester with a solvent system of *n*-hexane/2-propanol/trifluoroacetic acid (100:1:0.1, v/v/v) at a flow rate of 0.1 ml/min. *B*, CP-HPLC analysis of 9-HODE isolated by SP-HPLC separation of the CspLOX2 reaction products with a solvent system of *n*-hexane/2-propanol/trifluoroacetic acid (100:5:0.1, v/v/v) at a flow rate of 0.1 ml/min. *C*, CP-HPLC analysis of 13-HODE isolated by SP-HPLC separation of the CspLOX2 reaction products with a solvent system of *n*-hexane/2-propanol/trifluoroacetic acid (100:5:0.1, v/v/v) at a flow rate of 0.1 ml/min.

Besides the endogenous substrate 18:2(n-6), CspLOX2 could also metabolize other PUFAs, such as 18:3(n-3) and 20:4(n-6). Again three products were identified: 11-, 9-, and 13-H(P)OTE and 13-, 11-, and 15-H(P)ETE, respectively (supplemental Fig. S2 and Table S1). For 18:3(n-3) three additional products were detected. Two of these exhibited the characteristic spectrum of a conjugated triene chromophore and MS^2 spectra were previously described (35). Therefore the two compounds were identified as diastereomers of 9,16-dihydroxyoctadecatrienoic acid (9,16-diHOTE). The third product was identified as 9-KOTE (absorbance maximum at 274 nm in SP-HPLC solvent and MS^2 signals as described in Ref. 36). These products were formed from 9*R*-HPOTE: Upon incubation of CspLOX2 with the hydroperoxide absorbance at 234 nm decreased and at the same time absorbance at 269 nm appeared (supplemental Fig. S3*A*). RP-HPLC/MS^2 analysis confirmed the presence of the three products, the 9,16-diHOTE diastereomers (supplemental Fig. S3*B*, *peaks 1 and 2*) and 9-KOTE (supplemental Fig. S3*C*, *peak 4*). Additionally, minor amounts of a fourth substance were detected (supplemental Fig. S3*B*, *peak 3*). The substance was tentatively assigned as 11-hydroxy-9,10-epoxyoctadecadienoic acid by its fragmentation pattern as described previously (37).

Stereospecificity of Hydrogen Abstraction—To establish the stereochemistry of hydrogen abstraction [(11*S*)-^{2}H]-18:2(n-6) was used as substrate. The observed mass of the reaction product was as in the case of the unlabeled 18:2(n-6) *m/z* 295, indicating that the pro-*S* hydrogen was abstracted from the fatty acid. When the labeled fatty acid was used as substrate, the amount of the bisallylic 11*R*-HODE formed was reduced drastically and consisted of less than 1% of total reaction products, probably because of a deuterium primary isotopic effect.

Rearrangement of the Bisallylic Hydroperoxide by CspLOX2—To elucidate whether CspLOX2 can rearrange the detected 11-hydroperoxide to a conjugated product, as has been described for the Mn-LOX, 11*R*-HPODE was incubated with
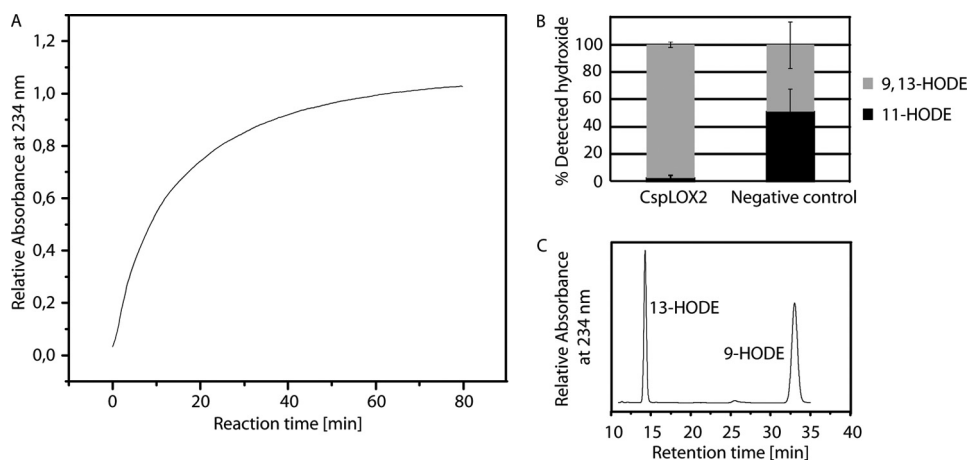
FIGURE 4. **Isomerization of 11-HPODE to hydroperoxides having conjugated diene systems by CspLOX2.** *A*, increase in UV absorbance at 234 nm during incubation of 4 mg of CspLOX2 with 11-HPODE in 200 mM sodium borate pH 9.5. *B*, relative hydroxide amounts after incubation of 11-HPODE with CspLOX2. The hydroperoxide was incubated at room temperature for 30 min in the presence and absence of CspLOX2. Hydroperoxides were reduced with SnCl$_2$, extracted, and analyzed by RP-HPLC/MS^2. The figure shows mean values and standard deviations, which were calculated from three independent experiments. *C*, SP-HPLC analysis of the produced HODEs having conjugated diene systems.

purified protein. Diene formation was followed at 234 nm and an increase was observed (Fig. 4*A*). Hydroperoxides were reduced, extracted and analyzed by RP-HPLC/MS^2. In parallel a preparation without the addition of enzyme was analyzed as a negative control. In the presence of CspLOX2, a single peak could be detected with a UV absorbance showing a maximum at 234 nm. Further analysis of the peak revealed the presence of an equimolar mixture of 9*R*- and 13*S*-HODE (Fig. 4, *B* and *C*).

Kinetic Analysis of CspLOX2—For determination of the kinetic parameters of CspLOX2, the initial rate of oxygen consumption for different concentrations of 18:2(n-6) was monitored in 0.2 M sodium borate buffer pH 9.5 using a Clark-type O$_2$ electrode. Triplicate measurements were then fitted to a Michaelis-Menten plot. The maximal reaction rate of 18:2(n-6) conversion was calculated as 30.7 $\pm$ 1.5 s^{-1} while the K_m value was calculated as 18.0 $\pm$ 2.6 μM. Because 18:2(n-6) was converted to 39.2% 11-HODE, 33.5% 9-HODE, and 27.3% 13-HODE, the apparent rate of substrate oxygenation to the respective product was 12.0 s^{-1}, 10.3 s^{-1}, and 8.4 s^{-1}.

Metabolism of PC Esters—The ability of a LOX enzyme to utilize esterified fatty acids with a bulky head group (such as PC esters) as substrate has been implicated with the substrate binding orientation. In the case of a LOX boot-shaped binding site hypothesis it is assumed that a LOX reaction with such substrates is only possible, when fatty acid binding takes place with the methyl end first (38). For this reason we investigated the metabolism of PC-20:4(n-6) by CspLOX2. The reaction was carried out under previously described high enzyme and substrate conditions and required the use of sodium deoxycholate to facilitate substrate solubilization (23). The reaction products were transesterified to methyl esters. Indeed PC-20:4(n-6) was converted, in comparable amounts as the free fatty acid substrate, into a mixture of three products. Two of the peaks could be identified as 11-HETE and 15-HETE by comparison of elution time and MS fragmentation pattern to that of authentic standards (Fig. 5*A*). The third peak, which showed an absorbance maximum at

202 nm displayed a MS^2 fragmentation pattern which has previously been described for 13-HETE (39) (Fig. 5*B*). 13-HETE, 15-HETE, and 11-HETE were formed at 56.6, 12.9, and 30.6%, respectively. CP-HPLC revealed that 15-HETE and 11-HETE were chiral (Fig. 5*C*). From these results we conclude that fatty acid binding takes place with the methyl end first.

DISCUSSION

In this study we aimed to characterize CspLOX2, which is one of the two predicted LOX-related sequences found in the genome of the diazotrophic cyanobacterium *Cyanothece* sp. CspLOX2 was cloned and expressed in *E. coli*, and the recombinant enzyme was purified. We show that CspLOX2 is to our knowledge the first LOX that has an iron as active site metal and produces a bisallylic hydroperoxide, namely 11*R*-HPODE, as its major product, when 18:2(n-6) is used as substrate. Besides this product, upon incubation of CspLOX2 with 18:2(n-6) a mixture of typical LOX products 13*S*- and 9*R*-HPODE were formed. So far, the only LOXs that have been reported to produce bisallylic hydroperoxides are the Mn-LOX from the fungus *G. graminis* (10, 40) and the LOX domain of the allene oxide synthase-LOX fusion protein from the coral *Plexaura homomalla*, which formed the 10-hydroperoxide out of 20:3(n-6) (41). Mn-LOX is the best studied example of a bisallylic LOX and can convert 18:2(n-6) to 11*S*-HPODE and 13*R*-HPODE in a 1:3 ratio with the latter accumulating as an end product (40). Though CspLOX2 and Mn-LOX both produce bisallylic hydroperoxides they differ in a number of characteristics of catalysis.

Sequence homology suggests that CspLOX2 belongs to the class of mini-LOXs, which consist only of the C-terminal LOX catalytic domain of about 65 kDa and lack the N-terminal β-barrel or C2-like domain. These enzymes are significantly smaller than the described animal and plant LOXs and a number of them have so far been identified in cyanobacteria (35, 42–45). Alignment of the predicted amino acid sequence of CspLOX2 with that of Mn-LOX shows conserved features, *e.g.* the four metal ligands and significant differences: One of the unique features of Mn-LOX is that helix α9, which harbors two of the metal ligands, contains 28 amino acids with two single amino acid gaps in comparison with all other known LOX sequences. On the contrary, the corresponding helix of CspLOX2 contains 30 amino acids and can be aligned without gaps, though the sequence differs considerably from that of plant and animal LOXs (supplemental Fig. S1) (46). Additionally, on helix α18 that harbors the other two iron ligands, CspLOX2 carries the H*XXX*N*XX*Q motif that is conserved among all LOXs. However, Mn-LOX has a serine residue in the position of the glutamine.
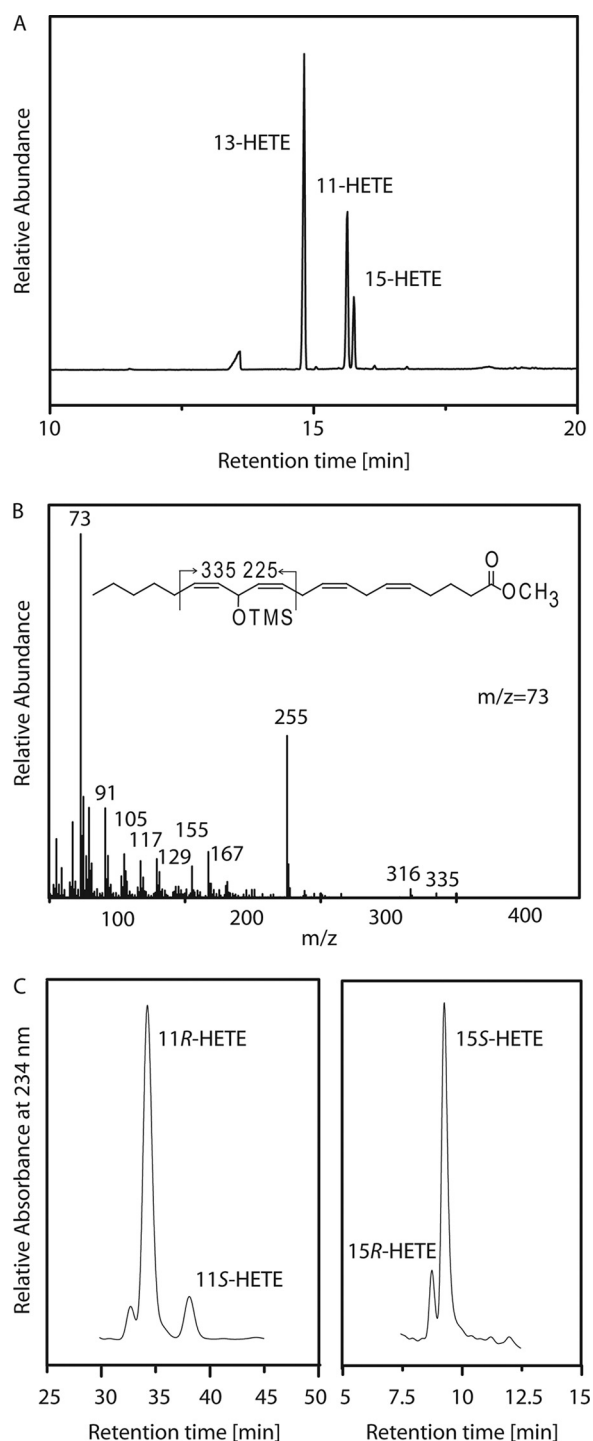
FIGURE 5. **Analysis of the products formed by CspLOX2 incubated with PC-20:4(n-6).** Enzyme preparation of CspLOX2 was incubated with PC-20:4(n-6) in 200 mM sodium borate pH 9.5. The reaction products were reduced and transmethylated. *A*, GC/MS analysis of the trimethylsilyl ether/methyl ester derivatives of the reaction products. *B*, electron impact mass spectrum of trimethylsilyl ether/methyl ester derivatives of 13-HETE. *C*, CP-HPLC analysis of conjugated HETE reaction products.

Analysis of the metal content of CspLOX2 showed that it contained ~0.9 atom of Fe per mol of enzyme, when sufficient amounts of Fe were present in the growth media. Similar stoichiometry has been reported for soybean LOXs, with an iron/enzyme ratio of 0.7–1.0, while for mammalian enzymes an even lower content has been described, *e.g.* 0.3–0.7 mol of iron/mol

of LOX (47). Mn-LOX on the other hand has been reported to contain 0.94 mol of manganese/mol of enzyme, while iron was below detection limit (40). Interestingly, we observed that upon expression of CspLOX2 under poor iron conditions, manganese can be incorporated in the active site. Therefore, CspLOX2 might be a useful tool to directly compare the influence of the metal ion on LOX catalysis.

As mentioned above, both CspLOX2 and Mn-LOX can produce significant amounts of bisallylic hydroperoxides. CspLOX2 converts 18:2(n-6) primarily to 11*R*-HPODE while, Mn-LOX produces the stereoisomer 11*S*-HPODE. The turnover rate of 18:2(n-6) by the two enzymes is similar with 31 s^{-1} in the case of CspLOX2 and 26 s^{-1} in the case of Mn-LOX (40). Bisallylic hydroperoxides remained for a long time elusive peroxidation products (48). Studies on lipid peroxidation by EPR have shown that this is not due to unfavorable product formation. In contrast, in the case of a free linoleyl radical, oxygenation takes place preferably on C11, because at this position spin density is the highest (49). Kinetic studies on linoleate autoxidation products, however, demonstrated that the 11-peroxyl radical undergoes a much more rapid β-fragmentation ($\sim 2 \times 10^6 \text{ s}^{-1}$) than conjugated 9- and 13-peroxy radicals (30 s^{-1}) (1, 50). This implies that in the case of 11-hydroperoxide formation by CspLOX2, an efficient H-donor exists in close proximity to C11, which converts the bisallylic peroxy radical to the corresponding hydroperoxide and therefore prevents β-fragmentation.

Both CspLOX2 and Mn-LOX can proceed to rearrange the 11-HPODE to produce conjugated hydroperoxides: A single end product, 13*R*-HPODE in the case of Mn-LOX (10) and a mixture of 9*R*- and 13*S*-hydroperoxides in the case of CspLOX2. Previous studies have shown that the metal centers of manganese and iron enzymes have otherwise similar properties (40). This rearrangement, however, has been suggested to be related to the higher redox potential of Mn^{3+} ($\text{Mn}^{2+} \leftrightarrows \text{Mn}^{3+} + e^-$, ~1.5 V *versus* $\text{Fe}^{2+} \leftrightarrows \text{Fe}^{3+} + e^-$, 0.77 V) (51). The only iron LOX that has so far been investigated with respect to its ability to rearrange bisallylic hydroperoxides is soybean LOX-1. However, it catalyzed 11-HPODE isomerization only at very high enzyme excess (250 μg/ml) (52) whereas in the case of CspLOX2, 4 μg/ml were found to be sufficient. On the other hand, the observed conversion was much slower than that reported for Mn-LOX. This enzyme has been shown to isomerize concentrations of bisallylic hydroperoxide similar to the ones used in our experiments (50 mM) in 6–7 min, while CspLOX2 required about 30 min, similarly to soybean LOX-1 (52). The slower reaction rate in the case of CspLOX2 supports the fact that the nature of the active site metal may indeed play a role in this reaction. Notably, while both Mn-LOX and soybean LOX-1 converted 11-HPODE to 13*R*-HPODE (10, 52), CspLOX2 produced of a mixture of 13*S*-HPODE and 9*R*-HPODE. The fact that CspLOX2 forms both 9*R*- and 13*S*-hydroperoxides in similar amounts, suggests that CspLOX2 may have no specific oxygen channel, which ensures oxygenation in a certain position of the fatty acid hydrocarbon chain. However, oxygen attack appears to take place only on one face of the substrate, suggesting that oxygen access on the other side may be hindered.
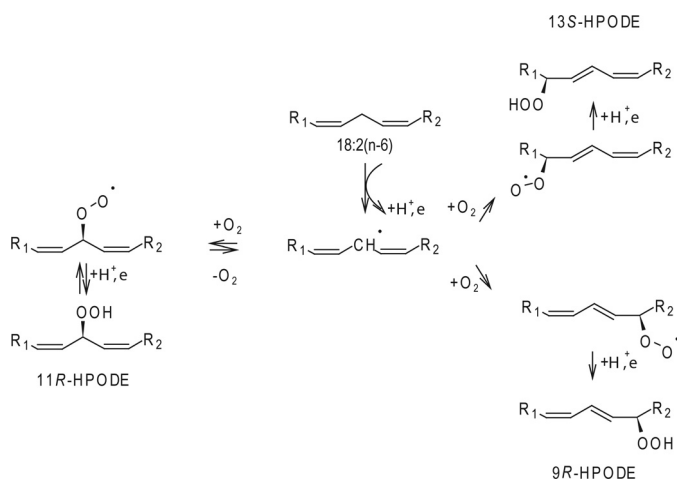
FIGURE 6. **Proposed mechanism for CspLOX2 with 18:2(n-6) as substrate.** The initiating step of catalysis is the abstraction of a bisallylic pro-*S* hydrogen from C11 of 18:2(n-6) leading to the formation of a radical. Oxygen is then reversibly inserted at position C11 and can be converted to 11*R*-HPODE. Oxygen can alternatively be inserted at C9 or C13 to irreversibly form 9*R*-HPODE and 13*S*-HPODE. As proposed by Ref. 10, free radical conversions are depicted.

Experiments with labeled [(11*S*)-²H]-18:2(n-6) suggest that CspLOX2 catalyzes an antarafacial oxygen insertion because no retention of deuterium in the formed products was observed. Antarafacial oxygenation has been previously reported for all LOXs, with the exception of Mn-LOX, which also abstracts the pro-*S* hydrogen from the C11 of 18:2(n-6), but subsequently catalyzes the oxygen insertion on the same side of the (1*Z*,4*Z*)-pentadiene system (10). The fact that the amounts of bisallylic hydroperoxide product were reduced when [(11*S*)-²H]-18:2(n-6) was used as CspLOX2 substrate may be indicative for a kinetically controlled formation of 11*R*-HPODE. A strong primary isotope effect was also described for Mn-LOX, but for this enzyme the proportion of the bisallylic hydroperoxide product remained unaltered regardless of the isotopically labeled 18:2(n-6) used as substrate (10).

Besides the endogenous PUFA substrate, 18:2(n-6), the specificity of CspLOX2 was tested with 18:3(n-3) and 20:4(n-6). In all cases CspLOX2 appears to abstract the (n-8) hydrogen and catalyzes stereospecific dioxygen insertions at positions (n-8), (n-6), and (n-10). Other than the case of Mn-LOX, CspLOX2 was able to convert both C18 and C20 PUFAs with a comparable reaction rate. These results suggest that fatty acids enter the enzyme active site with the methyl end first and that fixation of the carboxyl group of the fatty acid at a specific position is not essential for the reaction.

This mode of binding was also supported by the fact that CspLOX2 could react with PC-20:4(n-6) to produce the same oxygenated fatty acids that were found with free 20:4(n-6), with bisallylic 13-HPETE being the main product. The same mode of binding has been described for 13*S*-LOXs (53, 54), 9*R*-LOXs (23, 44), and Mn-LOX (51). On the other hand, a number of linoleate 9*S*-LOX and arachidonate 8*S*- and 5*S*-LOX cannot metabolize such substrates (55–57) and have been thought to bind fatty acids with the carboxylic end buried in the active site pocket. The production of the bisallylic product from esterified substrate has also been reported for Mn-LOX (51).

In summary, we describe a novel iron LOX, CspLOX2, that produces bisallylic hydroperoxides as its major products from all tested PUFA substrates. The substrates apparently bind to the active site with the methyl group first. With the endogenous fatty acid 18:2(n-6) CspLOX2 initially catalyzes the abstraction of the pro-*S* hydrogen from C11 and then the antarafacial oxygen insertion either reversibly to C11 forming the bisallylic hydroperoxide 11*R*-HPODE or irreversibly to C13 or C9 producing 13*S*-HPODE and 9*R*-HPODE, respectively (Fig. 6). All in all, CspLOX2 may be a suitable enzyme for structural studies to further study and understand the underlying mechanism that leads to the formation of bisallylic hydroperoxides.

REFERENCES

1. Schneider, C., Pratt, D. A., Porter, N. A., and Brash, A. R. (2007) *Chem. Biol.* **14,** 473–488
2. Kühn, H., Saam, J., Eibach, S., Holzhütter, H. G., Ivanov, I., and Walther, M. (2005) *Biochem. Biophys. Res. Commun.* **338,** 93–101
3. Andreou, A., Brodhun, F., and Feussner, I. (2009) *Prog. Lipid Res.* **48,** 148–170
4. Kühn, H., and Thiele, B. J. (1995) *J. Lipid Mediat. Cell Signal.* **12,** 157–170
5. Shureiqi, I., and Lippman, S. M. (2001) *Cancer Res.* **61,** 6307–6312
6. Kühn, H., Römisch, I., and Belkner, J. (2005) *Mol. Nutr. Food Res.* **49,** 1014–1029
7. Andreou, A., and Feussner, I. (2009) *Phytochemistry* **70,** 1504–1510
8. Oliw, E. H. (2002) *Prostaglandins Other Lipid Mediat.* **68–69,** 313–323
9. Palmieri-Thiers, C., Canaan, S., Brunini, V., Lorenzi, V., Tomi, F., Desseyn, J. L., Garscha, U., Oliw, E. H., Berti, L., and Maury, J. (2009) *Biochim. Biophys. Acta* **1791,** 339–346
10. Hamberg, M., Su, C., and Oliw, E. (1998) *J. Biol. Chem.* **273,** 13080–13088
11. Sloane, D. L., Leung, R., Craik, C. S., and Sigal, E. (1991) *Nature* **354,** 149–152
12. Borngräber, S., Kuban, R. J., Anton, M., and Kühn, H. (1996) *J. Mol. Biol.* **264,** 1145–1153
13. Boyington, J. C., Gaffney, B. J., and Amzel, L. M. (1993) *Science* **260,** 1482–1486
14. Minor, W., Steczko, J., Stec, B., Otwinowski, Z., Bolin, J. T., Walter, R., and Axelrod, B. (1996) *Biochemistry* **35,** 10687–10701
15. Skrzypczak-Jankun, E., Amzel, L. M., Kroa, B. A., and Funk, M. O. (1997) *Proteins* **29,** 15–31
16. Skrzypczak-Jankun, E., Bross, R. A., Carroll, R. T., Dunham, W. R., and Funk, M. O., Jr. (2001) *J. Am. Chem. Soc.* **123,** 10814–10820
17. Youn, B., Sellhorn, G. E., Mirchel, R. J., Gaffney, B. J., Grimes, H. D., and Kang, C. (2006) *Proteins* **65,** 1008–1020
18. Gillmor, S. A., Villaseñor, A., Fletterick, R., Sigal, E., and Browner, M. F. (1998) *Nat. Struct. Biol.* **4,** 1003–1009
19. Choi, J., Chon, J. K., Kim, S., and Shin, W. (2008) *Proteins* **70,** 1023–1032
20. Oldham, M. L., Brash, A. R., and Newcomer, M. E. (2005) *Proc. Natl. Acad. Sci. U.S.A.* **102,** 297–302
21. Neau, D. B., Gilbert, N. C., Bartlett, S. G., Boeglin, W., Brash, A. R., and Newcomer, M. E. (2009) *Biochemistry* **48,** 7906–7915
22. Vogel, R., Jansen, C., Roffeis, J., Reddanna, P., Forsell, P., Claesson, H. E., Kuhn, H., and Walther, M. (2010) *J. Biol. Chem.* **285,** 5369–5376
23. Andreou, A. Z., Vanko, M., Bezakova, L., and Feussner, I. (2008) *Phytochemistry* **69,** 1832–1837
24. Hamberg, M., Gerwick, W. H., and Åsen, P. A. (1992) *Lipids* **27,** 487–493
25. Rippka, R., Deruelles, J., Waterbury, J. B., Herdman, M., and Stanier, R. Y. (1979) *J. Gen. Microbiol.* **111,** 1–61
26. Hornung, E., Pernstich, C., and Feussner, I. (2002) *Eur. J. Biochem.* **269,**

4852–4859

27. Murray, M. G., and Thompson, W. F. (1980) *Nucleic Acids Res.* **8,** 4321–4325

28. Bligh, E. G., and Dyer, W. J. (1959) *Can. J. Biochem. Physiol.* **37,** 911–917

29. Brodhun, F., Göbel, C., Hornung, E., and Feussner, I. (2009) *J. Biol. Chem.* **284,** 11792–11805

30. Axelrod, B., Cheesbrough, T. M., and Laakso, S. (1981) *Methods Enzymol.* **71,** 441–451

31. Liavonchanka, A., Rudolph, M. G., Tittmann, K., Hamberg, M., and Feussner, I. (2009) *J. Biol. Chem.* **284,** 8005–8012

32. Lang, I., and Feussner, I. (2007) *Phytochemistry* **68,** 1120–1127

33. Koeduka, T., Kajiwara, T., and Matsui, K. (2007) *Curr. Microbiol.* **54,** 315–319

34. Oliw, E. H., Su, C., Skogström, T., and Benthin, G. (1998) *Lipids* **33,** 843–852

35. Lang, I., Göbel, C., Porzel, A., Heilmann, I., and Feussner, I. (2008) *Biochem. J.* **410,** 347–357

36. Cristea, M., and Oliw, E. H. (2006) *J. Biol. Chem.* **281,** 17612–17623

37. Oliw, E. H., Garscha, U., Nilsson, T., and Cristea, M. (2006) *Anal. Biochem.* **354,** 111–126

38. Coffa, G., Schneider, C., and Brash, A. R. (2005) *Biochem. Biophys. Res. Commun.* **338,** 87–92

39. Brodowsky, I. D., and Oliw, E. H. (1993) *Biochim. Biophys. Acta* **1168,** 68–72

40. Su, C., Sahlin, M., and Oliw, E. H. (2000) *J. Biol. Chem.* **275,** 18830–18835

41. Boutaud, O., and Brash, A. R. (1999) *J. Biol. Chem.* **274,** 33764–33770

42. Gao, B., Boeglin, W. E., and Brash, A. R. (2010) *Biochim. Biophys. Acta* **1801,** 58–63

43. Schneider, C., Niisuke, K., Boeglin, W. E., Voehler, M., Stec, D. F., Porter, N. A., and Brash, A. R. (2007) *Proc. Natl. Acad. Sci. U.S.A.* **104,** 18941–18945

44. Zheng, Y., Boeglin, W. E., Schneider, C., and Brash, A. R. (2008) *J. Biol. Chem.* **283,** 5138–5147

45. Gao, B., Boeglin, W. E., Zheng, Y., Schneider, C., and Brash, A. R. (2009) *J. Biol. Chem.* **284,** 22087–22098

46. Prigge, S. T., Boyington, J. C., Gaffney, B. J., and Amzel, L. M. (1996) *Proteins* **24,** 275–291

47. Aleem, A. M., Jankun, J., Dignam, J. D., Walther, M., Kühn, H., Svergun, D. I., and Skrzypczak-Jankun, E. (2008) *J. Mol. Biol.* **376,** 193–209

48. Brash, A. R. (2000) *Lipids* **35,** 947–952

49. Kitaguchi, H., Ohkubo, K., Ogo, S., and Fukuzumi, S. (2005) *J. Am. Chem. Soc.* **127,** 6605–6609

50. Tallman, K. A., Pratt, D. A., and Porter, N. A. (2001) *J. Am. Chem. Soc.* **123,** 11827–11828

51. Oliw, E. H. (2008) *J. Lipid Res.* **49,** 420–428

52. Oliw, E. H., Cristea, M., and Hamberg, M. (2004) *Lipids* **39,** 319–323

53. Feussner, I., Balkenhohl, T. J., Porzel, A., Kühn, H., and Wasternack, C. (1997) *J. Biol. Chem.* **272,** 21635–21641

54. Gardner, H. W. (1989) *Biochim. Biophys. Acta* **1001,** 274–281

55. Andreou, A. Z., Hornung, E., Kunze, S., Rosahl, S., and Feussner, I. (2009) *Lipids* **44,** 207–215

56. Boeglin, W. E., Itoh, A., Zheng, Y., Coffa, G., Howe, G. A., and Brash, A. R. (2008) *Lipids* **43,** 979–987

57. Jisaka, M., Kim, R. B., Boeglin, W. E., and Brash, A. R. (2000) *J. Biol. Chem.* **275,** 1287–1293